Solvent-Dependent Dihydrogen/Dihydride Stability for [Mo(CO)(Cp*)H2(PMe3)2]+[BF4]− Determined by Multiple Solvent···Anion···Cation Non-Covalent Interactions

Pavel Dub, Natalia V Belkova, Oleg A Filippov, Jean-Claude Daran, Lina M Epstein, Agusti Lledos, Elena S. Shubina, Rinaldo Poli

DOI: 10.1002/chem.200((……))

Solvent-Dependent Dihydrogen/Dihydride Stability for $[Mo(CO)(Cp^*)H_2(PMe_3)_2]^+[BF_4]^-$ Determined by Multiple Solvent···Anion···Cation Non-Covalent Interactions

Pavel A. Dub,[a,b] Natalia V. Belkova,[b] Oleg A. Filippov,[b] Jean-Claude Daran,[a] Lina M. Epstein,[b] Agustí Lledós,[c] Elena S. Shubina,*[b] Rinaldo Poli*[a,d]

Abstract: Low temperature (200K) protonation of compound $[Cp^*Mo(PMe_3)_2(CO)H]$, **1**, by $Et_2O{\cdot}HBF_4$ yields a different result depending on a subtle solvent change: the dihydrogen complex $[Cp^*Mo(PMe_3)_2(CO)(\eta^2\text{-}H_2)]^+$, **2**, is obtained in THF, whereas the tautomeric classical dihydride $[Cp^*Mo(PMe_3)_2(CO)(H)_2]^+$, **3**, is the only observable product in dichloromethane. Both products were fully characterized (ν_{CO} IR, ^1H, ^{31}P, ^{13}C NMR) at low temperature; they loose H_2 upon warming to 230 K at approximately the same rate of ca 10^{-3} s^{-1} (with no detection of the non-classical form in CD_2Cl_2), generating $[Cp^*Mo(PMe_3)_2(CO)(FBF_3)]$, **4**. The latter also slowly decomposes at ambient temperature. One of the decomposition products was crystallized and identified by X-ray crystallography as $[Cp^*Mo(PMe_3)_2(CO)(FH\cdots FBF_3)]$, **5**, featuring a neutral HF ligand coordinated to a transition metal through the F atom and to the BF_4^- anion through a hydrogen bond. The reason for the switch of relative stability between **2** and **3** was probed by DFT calculations based on the B3LYP and M05-2X functionals, with inclusion of anion and solvent effects through the conductor-like polarizable continuum model (CPCM) and by the explicit consideration of solvent molecules. Calculations at the MP4(SDQ) and CCSD(T) levels on the simplified $[CpMo(PH_3)_2(CO)H_2]^+$ model were also carried out for calibration. The calculations reveal the key role of non covalent anion-solvent interactions, which modulate the anion-cation interaction ultimately altering the energetic balance between the two isomeric forms.

Keywords: Molybdenum · hydride ligands · dihydrogen complexes · proton transfer · DFT calculations · solvent effects · non covalent interaction

Introduction

After the discovery of the first isolable transition metal dihydrogen complex by Kubas and co-workers,[1] this important class of coordination compounds spread rapidly into an active field of study.[2] Together with mono- or polyhydride complexes, dihydrogen complexes play an important role in many homogeneous catalytic processes.[3] The most common methods to generate $(\eta^2\text{-}H_2)$-complexes are (a) addition of H_2 gas to an unsaturated precursor, (b) ligand displacement by H_2 gas, and (c) protonation of a hydride complex,[4] the latter being the simplest and most convenient method. Protonation of neutral hydride compounds most often leads to the kinetically controlled proton addition to a metal hydride, forming either a dihydrogen complex $M(\eta^2\text{-}H_2)$, or a *cis*-dihydride, $M(H)_2$, depending on the nature of the metal and ligands.[5] Recently, the low temperature protonation of [Cp*M(dppe)H] was shown to produce $[Cp^*M(dppe)(\eta^2\text{-}H_2)]^+$ for M = Fe[6] or Ru[7] and [*cis*-$Cp^*M(dppe)(H)_2]^+$ for M = Os.[8] When a dihydrogen complex $M(\eta^2\text{-}H_2)$ is initially formed, its ultimate fate depends on the metal electronic properties: it is stable when the metal has suitable Lewis acidity and π back-bonding ability; it isomerizes to a polyhydride structure if the metal has a strong back-donating power; and it will evolve H_2 if there is insufficient back-donation.

When a neutral hydride complex is protonated, the nature of the solvent may be expected to have a profound effect on the outcome through the effects of polarity (defined herein by the dielectric

[a] Mr. Pavel Dub, Dr. Jean-Claude Daran, Prof. Rinaldo Poli
CNRS; LCC (Laboratoire de Chimie de Coordination);
Université de Toulouse; UPS, INPT;
205, route de Narbonne, F-31077 Toulouse
Fax: +33-561553003
E-mail: rinaldo.poli@lcc-toulouse.fr

[b] Dr. Natalia V. Belkova, Dr. Oleg A. Filippov, Prof. Lina M. Epstein, Prof. E. S. Shubina
A. N. Nesmeyanov Institute of Organoelement Compounds,
Russian Academy of Sciences,
Vavilov Street 28, 119991 Moscow, Russia

[c] Prof. Agustí Lledós
Departament de Química, Edifici Cn,
Universitat Autónoma de Barcelona, 08193 Bellaterra, Spain

[d] Institut Universitaire de France,
103, bd Saint-Michel, 75005 Paris, France

Supporting information for this article is available on the WWW under http://www.chemeurj.org/ or from the author.

permittivity) and/or the possible establishment of specific interactions (H-bonding) with the neutral solutes (hydride complex, proton donor) or with the proton transfer product.[9] Few previous contributions have specifically addressed solvent effects on the protonation process of neutral hydride complexes. For instance, the low-temperature protonation of $[Cp^*RuH_3(PCy_3)]$ by R_FOH (hexafluoroisopropanol or perfluoro-*tert*-butanol), yielding $[Cp^*Ru(H)_2(\eta^2\text{-}H_2)(PCy_3)]^+[ORF]^-$, is assisted by the Freon mixture relative to toluene, because of the dielectric constant increase upon cooling.[10] The protonation kinetics of complex $[W_3S_4(dmpe)_3H_3]^+$ is also affected by the solvent (MeCN vs. CH_2Cl_2).[11] The solvent polarity effect on the proton transfer thermodynamics and energy barrier has been shown for the protonation of $[CpRuH(CO)(PCy_3)]$[12] and $[Ru(PP_3)H_2]$[13] [PP_3 = $P(CH_2CH_2PPh_2)_3$]. For the latter system, the ability of the H-bond donating solvent to interfere with the formation of H-bonds in the [M-H···H-A] and $[M(H_2)^+\cdots A^-]$ species was demonstrated. More recently, we have shown that the protonation of $Cp^*Mo(dppe)H_3$ by CF_3COOH can be directed toward the formation of either $[Cp^*Mo(dppe)H_4]^+$ or $[Cp^*Mo(dppe)H_2(O_2CCF_3)]$ depending on the solvent ability to separate the initially formed $[Cp^*Mo(dppe)H_4]^+(CF_3COO^-)$ contact ion pair.[14]

From those studies it is clear that the proton transfer rate and equilibrium position are sensitive to a complex combination of interactions of various nature such as hydrogen bond, ion pair, electrostatic, weak forces etc… The same forces could influence the preference for the classical *vs*. non-classical isomers, but up to date there is no example of switching such preference depending on the conditions. In the present contribution, we report the first direct observation of a solvent influence on the classical vs non-classical nature of the protonation product and a computational study that rationalizes this phenomenon.

Results

(a) Proton transfer to compound 1 at low temperatures

A previously reported room temperature protonation study of complex $[Cp^*Mo(CO)(PMe_3)_2H]$, **1**, by RCO_2H (R = H, Me, Et) was shown[15] to directly afford $Cp^*Mo(PMe_3)_2(CO)(\eta^1\text{-}O_2CR)$ and H_2, presumably via an initial (unobserved) intermediate $(\eta^2\text{-}H_2)$-complex. We now report our studies of the protonation of **1** by $Et_2O{\cdot}HBF_4$ at room and low (193 K) temperatures in solvents possessing close polarity and different coordinating ability (THF and CH_2Cl_2), using IR (ν_{CO}) and NMR (^1H, $^{31}P\{^1H\}$, $^{13}C\{^1H\}$) spectroscopic methods. Like many other hydride complexes, **1** is not stable in CH_2Cl_2 at ambient temperature, slowly undergoing H/Cl exchange (ca. 11% conversion in 26 hours),[16] but this reaction does not take place at any measurable rate at low temperatures, allowing us to carry out low temperature studies in this solvent.

Addition of a stoichiometric amount of $Et_2O{\cdot}HBF_4$ to a pale orange solution of **1** in benzene or THF at ambient temperatures yields an immediate color change to deep-purple and gas evolution. The ^1H and $^{31}P\{^1H\}$ NMR spectra showed complete consumption of the starting material and formation of new nonhydridic products (no resonances upfield of TMS). When the $Et_2O{\cdot}HBF_4$ addition was carried out at 200K in THF-d_8, however, the selective formation of the dihydrogen complex $[Cp^*Mo(CO)(PMe_3)_2(\eta^2\text{-}H_2)]^+$ (**2**) was observed, see Figure 1. This is suggested by the broad shape of the hydride resonance at -5.14 ppm in the ^1H NMR spectrum and confirmed by the low T_{1min} value of 24 ms at 190K (500 MHz). Application of the method of Halpern and co-workers gives an H-H distance of 1.1 Å in the slow rotation regime[17], or 0.88 Å in the fast rotation regime.[18] Other selected NMR and IR properties of this compound can be found in Table 1 together with those of the starting material, whereas the complete characterization is provided as Supporting Information.

A parallel experiment with IR monitoring (ν_{CO}-region) showed the growth, after the acid addition, of a new band ν_{CO} at 1852 cm^{-1}, attributed to the dihydrogen complex **2** (see Figure 2). The high-frequency shift ($\Delta\nu$ = +76 cm^{-1}) is in accord with a significant lowering of the M $d(\pi) \rightarrow$ CO ($p\pi^*$) back-donation upon protonation.[19] Upon raising the temperature to 230 K the hydride resonance in the NMR spectrum gradually disappeared while H_2 evolved, as shown by the characteristic ^1H NMR resonance at δ 4.58. Correspondingly the intensity of the ν_{CO}(**2**) band in the IR spectrum decreased, while a new ν_{CO} band appeared at 1800 cm^{-1}. The new compound (**4**) is characterized by a $^{31}P\{^1H\}$ NMR resonance at δ 19.4 and by ^1H NMR resonances at δ 1.85 for Cp* and 1.48 for the two PMe_3 ligands at 230 K in THF-d_8. No resonance was observed for this compound in the hydride region. The nature of this product will be addressed in a later section.

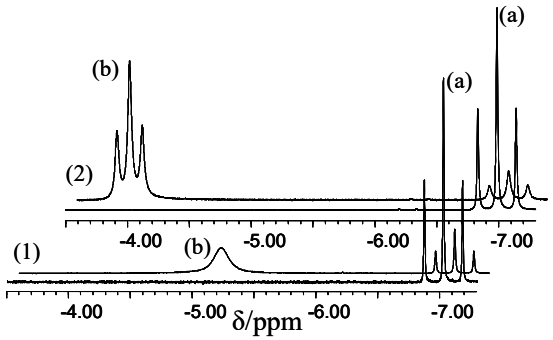

Figure 1. ^1H NMR (500 MHz) spectra in THF-d_8 (1) or CD_2Cl_2 (2) of: (a) compound 1 alone; (b) compound 1 in the presence of slightly less than 1 equiv of $Et_2O{\cdot}HBF_4$. [1] = 0.04 M; T = 200 K.

Table 1. Selected NMR and IR data for compounds **1**, **2** and **3** at 200K.

Compd	Solv.	δ hydride[a]	T_{1min}/ms (T/K)	δ PMe_3[b]	δ CO[c]	ν_{CO}/ cm^{-1}
1	THF-d_8	-7.03 (t, 77)	882 (190)[d]	32.0 (s)	252.4 (t, 29)	1776
	CD_2Cl_2	-6.98 (t, 77)		31.4 (s)	255.0 (t, 29)	1751
2	THF-d_8	-5.14 (bs)	24 (190)	16.8 (s)	243.9[e]	1852
3	CD_2Cl_2	-3.92 (t, 55)	300 (190)	10.0 (s)	231.5 (t, 10)	1954

[a] ^1H NMR, multiplicity and J_{HP}/Hz in parentheses. [b] $^{31}P\{^1H\}$ NMR, multiplicity in parentheses. [c] $^{13}C\{^1H\}$ NMR, multiplicity and J_{CP}/Hz in parentheses. [d] In toluene-d_8. [e] No information on the multiplicity could be obtained.

Quite surprisingly, protonation of **1** with $HBF_4{\cdot}Et_2O$ in CD_2Cl_2 at 200K yielded completely different spectroscopic changes relative to those described above in THF, consistent with formation of the dihydride complex $[Cp^*Mo(PMe_3)_2(CO)(H)_2]^+$, **3**, see Figure 1 and Table 1. The hydride ligands exhibit only one triplet resonance at δ -3.92 with a T_{1min} value of 300 ms at 190K (500 MHz). A parallel IR experiment revealed a ν_{CO} band for **3** at 1954 cm^{-1}, at a much higher frequency ($\Delta\nu_{CO}$ = +203 cm^{-1}) relative to **2**, in agreement with the formally higher oxidation state in the classical structure. Similar trends in ν_{CO} shifts upon formation of non-classical and classical

dihydride derivatives were observed for the protonation of $Cp^*Os(CO)_2H$.[20] The thermal behaviour of **3** is identical to that of **2**: warming the sample to 230 K resulted in H_2 evolution (H_2 resonance at δ 4.64) to give **4**. The dihydrogen complex – a possible intermediate of the H_2 evolution process, was not observed in this solvent. Such a subtle solvent control of the classical/non-classical equilibrium is unprecedented, to the best of our knowledge.

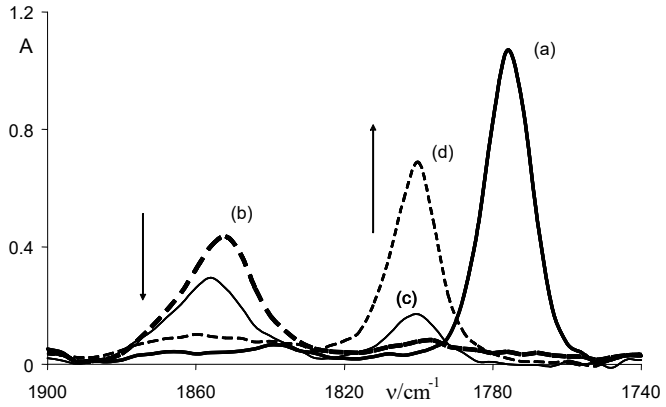

Figure 2. IR spectra in the ν_{CO} region of compound **1** in THF (C = $1.2 \cdot 10^{-2}$ M, l = 0.4 mm, 4 cm^{-1} resolution): (a) alone, at 200K; (b) in the presence of ca. 1 eq $HBF_4 \cdot Et_2O$, at 200K; (c) after warming to 230K (ca. 10 min after spectrum b); (d) 3 min after (c).

The observation of a single hydride resonance for **3** indicates that the compound either adopts a structure with two equivalent hydrides or that they undergo rapid mutual exchange on the NMR time scale. The related compounds $[CpMo(PMe_3)_3H_2]^+$ and $[Cp^*Mo(PMe_3)_3H_2]^+$ display averaged resonances at ambient temperature, which decoalesce at low temperatures, in agreement with structure **I** (L = PMe_3; R = H or Me).[21] Analogous structures were shown by X-ray crystallography for the isoelectronic compounds $[CpMo(PMe_3)_3(MeCN)H]^{2+}$, $[CpW(PMe_3)_2(CO)H_2]^+$ and $[(C_6H_5Me)W(PMe_3)_3H_2]^{2+}$,[20-21, 22] and was also proposed for $[CpMo(dppe)(CO)H_2]^+$ which, like our complex **3**, shows only one hydride resonance at low temperatures.[23] Therefore, we presume that structure **I** (L = CO; R = Me) is also adopted for compound **3**. As will be shown in a later section, the computational work confirms the lower energy of this geometry.

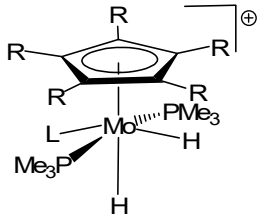

I

On the basis of the NMR results alone, one could not conclude that the reaction selectively yields a different product in each solvent, because rapid interconversion (see the theoretical section below for an estimation of the barrier) would result in a single resonance under all circumstances. However, the much faster IR experiment can distinguish isomers with much shorter lifetimes. No observable IR absorption for the nonclassical isomer **2** was observed in the CH_2Cl_2 experiment (see Supporting Information, Figure S1) and, likewise, no significant IR intensity for the classical isomer **3** was observed in the THF experiment (supplemental Figure S2). Given the signal-to-noise ratio of the IR experiment, we can conservatively estimate that < 5% of **2** is present in the CH_2Cl_2 solution of **3** (K = [**2**]/[**3**] < 0.053) and that < 5% of **3** is present in the THF solution of **2** (K > 24). This corresponds to a relative stability of the two isomers at 200K, on the free energy scale, of > 1.1 kcal mol^{-1} in favor of **3** in CH_2Cl_2 and > 1.1 kcal mol^{-1} in favor of **2** in THF.

Other interesting information was obtained from the $^{13}C\{^1H\}$ NMR spectra of the protonation products at 200 K. The CO resonance moves upfield by 8.5 ppm upon transforming **1** to **2**, whereas it moves upfield by 23.5 ppm upon transforming **1** to **3**. There is a good correlation between the ^{13}C shifts and ν_{CO} frequencies for these complexes in both THF and CH_2Cl_2 (Equation 1, $r^2 = 0.999$). Such correlations are known for various carbonyl complexes,[24] the ^{13}C shifts and ν_{CO} frequencies being function of the ligand substituent properties like e.g. for the complexes with a variety of 4-substituted pyridine ligands *cis*-$Mo(CO)_4$(py-4-X)[25] and Fe(TPP)(CO)(py-4-X),[26].

$$\delta(^{13}C) = -0.116\ \nu_{CO} + 458.34 \qquad (1)$$

(b) Theoretical study of the factors affecting the dihydrogen-dihydride equilibrium in the $[Cp^*Mo(CO)(PMe_3)_2H_2]^+$ system.

The computational investigation was motivated by the desire to understand the origin of the different isomeric preference in closely related solvents. All geometry optimizations were carried out by means of DFT calculations using both the standard B3LYP functional and the recently introduced[27] M05-2X functional. The latter was shown to give better results in studies of noncovalent interactions.[28] The internal geometries of the Mo complexes are quite functional-independent, the main difference being a systematic shortening of all distances on going from B3LYP to M05-2X [by ca. 0.05 Å for Mo-P, 0.02 Å for Mo-C(Cp), 0.01 Å for Mo-CO and C-O, 0.005 Å for C-C(ring) and C(ring)-CH_3]. Comparative structural details for the geometries optimized by the two different functionals are available in the Supporting Information (Tables S1-S4). Additional calculations on selected systems were carried out by MP2 and B3PW91 on the fixed B3LYP geometries (Table S5). The structural parameters henceforth reported refer only to the M05-2X calculations.

Among the two possible isomers of **1** with a *cis* or *trans* arrangement of the H and CO ligands, the latter was found more stable (by ΔE^g = -6.6 kcal mol^{-1}), in agreement with the experimentally suggested geometry. Only this isomer (Figure 3) was therefore considered in further calculations. Optimization of the non-classical complex **2** revealed two isomers having the H_2 ligand either parallel (see Figure S3 in the Supporting Information) or perpendicular (Figure 3) to the Cp* ring. The latter is lower in energy by 0.2 kcal mol^{-1}, but higher by 0.3 kcal mol^{-1} after ZPVE correction and by 0.6 kcal mol^{-1} on the free energy scale. Since most of the non-classical complexes optimized in this work (see below) have the H_2 ligand perpendicular to the Cp* ring, the perpendicular geometry was used as the reference. The energy minimum for the classical dihydride **3** corresponds to the expected pseudo-octahedral geometry (see **I**). Other local minima include a second pseudo-octahedral geometry with axial hydride and two *cis* PMe_3 ligands in the equatorial plane (+2.6 kcal mol^{-1} from **I**) and pseudo-pentagonal pyramids with either adjacent or non-adjacent PMe_3 ligands (+5.4 and +4.1 kcal mol^{-1}, respectively).[29] The most stable classical geometry of **3** has almost equal energy as the nonclassical isomer **2** in the gas phase (higher by only 1.4 kcal mol^{-1}), with a low $Mo(\eta^2\text{-}H_2) \rightarrow Mo(H)_2$

interconversion barrier (4.3 kcal mol^{-1}, see the transition state geometry in Figure S4). This low barrier is entirely consistent with the minor rearrangement of the coordination sphere during the isomerization. The proton affinity of the hydride **1** calculated as $-\Delta H_{298.15K}$ for the reaction **1** + $H^+ \rightarrow$ **2** is 242.6 kcal mol^{-1}. This gas-phase value gives a first indication of the high basicity of the hydride ligand of **1**.

The effects of the BF_4 counter-anion and solvent on the relative stability of **2** and **3** were evaluated by the explicit inclusion of the counterion as well as one or more solvent molecules, and by inclusion of the polarizability of the medium through the CPCM. The results on the relative energy are summarized in Table 2. The individual formation energies relative to the separate cation, anion and solvent, in gas phase (ΔE^g) and in solution (ΔE^{solv}) are available in the Supporting Information (Table S6).

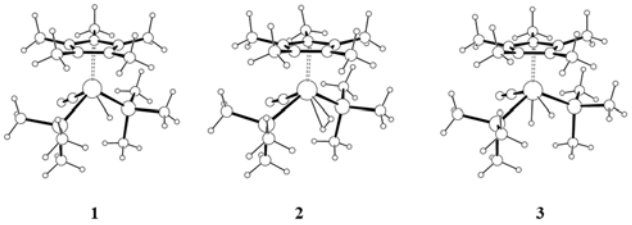

Figure 3. View of the M05-2X optimized geometries for complexes **1**, **2** and **3**.

An analysis of Table 2 immediately reveals that all the chosen models and computational levels do not provide quantitative agreement with the experimental evidence: the DFT methods predict greater stability for the nonclassical isomer under all conditions, except for a slight preference for the classical isomer in the case of the gas phase free cation at the B3PW91 level. The addition of the BF_4^- anion, or solvent molecule, or both, whether in the gas phase or in the presence of the appropriate CPCM, increase the relative stability of the nonclassical isomer, including in CH_2Cl_2 where a preference for the classical structure is shown experimentally. Conversely, the MP2 method overestimates the stability of the classical isomer. However, all calculations indicate a delicate energetic balance between the two isomers. Note that the addition of the solvent, both by the explicit inclusion of solvent molecules in the optimization and by consideration of the CPCM, increases the relative stability of the nonclassical isomer to a greater extent for THF than for CH_2Cl_2 (for instance the Ion-pair·$3CH_2Cl_2$ system shows a 5.9 kcal mol^{-1} preference for the nonclassical structure, whereas this preference increases to 7.4 kcal mol^{-1} for the Ion-pair·3THF system).

All CPCM calculations were carried out on the fixed geometries obtained from the gas-phase optimization. The possibility that the CPCM might significantly affect the geometry of the energy minimum was tested by fully reoptimizing the **2**BF_4 and **3**BF_4 geometries (only at the M05-2X level) in the presence of the CH_2Cl_2 and THF CPCM. The internal geometry of the cation was practically unaffected, whereas the cation-anion interactions became slightly looser (slightly longer H···F and shorter B-$F^{H\text{-}bond}$ distances), see Table S4. However, the energy differences in solution were not greatly affected (from +4.9 to +4.9 kcal mol^{-1} in CH_2Cl_2; from +4.8 to +4.6 kcal mol^{-1} in THF). Thus, we wondered whether there may be an inherent bias in favor of the nonclassical structure by the DFT method and in favor of the classical one by MP2.

Geometry optimizations at higher level are prohibitive for this system. Thus, calibration tests were carried out at the MP4(SDQ) and CCSD(T) levels using the MP2 optimized geometries of the $[Cp^*Mo(CO)(PMe_3)_2H_2]^+$ systems only as free ions in the gas phase, as well as the MP2, B3LYP, B3PW91 and M05-2X levels with full geometry optimization. These calculations yielded the following values for E^g(**3**)-E^g(**2**): +0.1 (B3LYP), -1.0 (B3PW91), +1.3 (M05-2X), -8.4 (MP2), -4.1 (MP4(SDQ)), and -3.7 (CCSD(T)). For this system, the higher-level MP4(SDQ) and CCSD(T) calculations yield essentially identical results, suggesting greater stability for dihydride complex by ca. 3 kcal mol^{-1} relative to the dihydrogen isomer. This results are half-way between those of the DFT methods, which overestimate the stability of the dihydrogen complex by 4-5 kcal/mol, and that of MP2, which overestimates the stability of the dihydride by the same amount. If we apply this 4-5 kcal/mol correction to the values shown in Table 2, these become in good agreement with the experimental observation. Thus, this calibration test is in agreement with the bias of DFT in favour of the non classical structure and of MP2 in favour of the classical one.

The remainder of this section will focus on a more detailed analysis of the effects introduced by anion and solvent on the structure and energetics properties, giving a clue as to how the solvent operates for switching the cation isomeric preference. The effects of anion and solvent on selected IR spectral parameters (ν_{HH}, ν_{MH} and ν_{CO}) are analyzed in the Supporting Information section (Tables S7 and S8).

Ion-pairing. Calculations show that in the gas phase, as well as in solution, the ion-pair interaction dominates over the solvent-cation and solvent-anion interactions, in agreement with the presence of the ion-pair in low polarity solvents, rather than the separated solvated ions (formation energies for cation·solvent, anion·solvent and cation·anion are collected in Table S6). The calculations also

Table 2. Relative stability of the dihydrogen and dihydride isomers, using different models.

Model	Gas phase[a]				CPCM (CH_2Cl_2)[b]		CPCM (THF)[b]	
	M05-2X	B3LYP	B3PW91[c]	MP2[c]	M05-2X	B3LYP	M05-2X	B3LYP
cation	+1.3(+1.0)	+0.1	-1.0	-9.6	+2.2(+1.8)	+0.5	+2.1(+1.8)	+0.4
cation·CH_2Cl_2	+2.4(+1.5)	+0.8			+3.2(+2.4)	+0.7		
cation·THF	+3.2(+2.3)	+1.1					+3.9(+3.0)	+0.7
Ion-pair	+5.9(+6.0)	+5.3	+4.6	-4.2	+4.9(+5.0)	+4.1	+4.8(+4.9)	+4.0
Ion-pair·CH_2Cl_2	+5.5(+4.2)	+4.5	+3.8	-5.0	+5.5(+4.1)	+4.2		
Ion-pair·THF	+6.9(+8.0)	+5.5	+4.8	-1.8			+5.9(+7.0)	+4.2
Ion-pair·$3CH_2Cl_2$	+6.6(+8.3)				+5.9(+7.5)			
Ion-pair·3THF	+8.8(+9.5)						+7.4(+8.1)	

[a] The reported values are ΔE [E(**3**)–E(**2**)] in kcal/mol, with ΔG [G(**3**)–G(**2**)] in parentheses. [b]The CPCM results were obtained at the fixed geometry from the gas phase optimization. The reported values are ΔE^{solv} in kcal/mol, with ΔG^{solv} in parentheses. The latter have been obtained by adding the gas phase free energy corrections on the solute to ΔE^{solv}. [c]The B3PW91 and MP2 calculations were carried out at the fixed B3LYP-optimized geometry.

demonstrate that the presence of the counter-anion modifies significantly the classical-nonclassical equilibrium in favour of the dihydrogen complex (by 4.5 kcal mol^{-1} at the M05-2X level and by 5.4 kcal mol^{-1} at the MP2 level in the gas-phase). This effect is probably related to a stronger cation-anion interaction for **2**BF_4, as suggested by the shorter F···H contacts (see Figure 4). For both **2**BF_4 and **3**BF_4, many of these F···H contacts are substantially shorter than the sum of van der Waals radii (2.55 Å), but those found in **2**BF_4 are on average shorter than those of **3**BF_4. Note that the F···H separations involving the dihydrogen ligand in **2**BF_4 are close to the shortest distances implicating the Cp* and PMe_3 hydrogen atoms (ca. 2.1 Å). On the other hand, the F···H(Mo) contacts in **3**BF_4 (> 2.3 Å) are longer than the F···H(C) contacts (ca. 2.0 Å, see Figure 4).

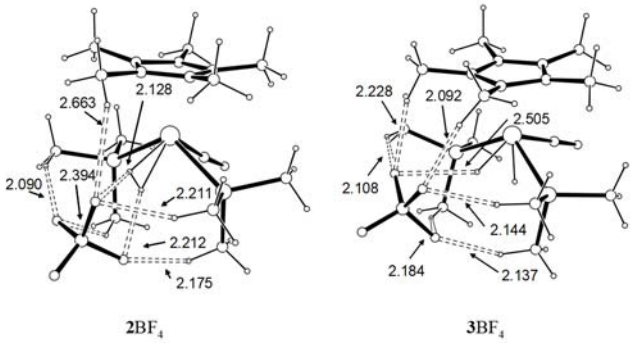

Figure 4. View of the M05-2X optimized geometries for the ion pairs 2BF_4 and 3BF_4.

Bulk solvent effects. Calculations prove that the solvent, described as a continuum, plays a minor role in discriminating the two isomers, as could have been anticipated from the very similar dielectric constant (THF: ε = 7.58; CH_2Cl_2: ε = 8.93). Both solvents stabilize **2** by 0.7 kcal/mol, while **2**BF_4 is disfavoured by 1.0 kcal/mol in CH_2Cl_2 and by 1.1 kcal/mol in THF (M05-2X values). Although the continuum decreases the preference for **2**BF_4, ion-pairing is still providing greater stabilization to **2**. Of course, depending on the relative stability of the two isomers of the isolated cation, the ion-pair formation in solution will reverse or not the energy ordering. However, bulk solvent effects alone are not able to explain the different behaviour in THF and CH_2Cl_2.

Discrete solvent effects. The explicit addition of solvent molecule(s) (either CH_2Cl_2 or THF) to the ion pair model engenders additional non covalent interactions with the anion, solvent···anion···cation, rather than with the cation, and involves the solvent C-H bonds as proton donors. Therefore, any effect on the cation stabilization must be indirect, through a modulation of the noncovalent cation-anion interaction through the noncovalent solvent-anion interaction(s). The relative cation-anion orientation is only slightly disturbed by the solvent addition, without significant lengthening the F···H(C) interactions (see supplementary Tables S3 and S4), whereas the solvent-anion (C)H···F interactions are significantly longer (by ca. 0.1 Å for CH_2Cl_2 and by ca. 0.2 for THF) than in the absence of cation (Table S4). No clear trend could be identified in the internal structure of the Mo complexes (classical or nonclassical). Both M05-2X and MP2 calculations show that the interaction of the ion-pair with THF stabilizes **2**BF_4 (by 1.0 and 2.4 kcal mol^{-1} at the M05-2X and MP2 levels, respectively). The interaction with CH_2Cl_2 has less influence in the relative stabilities and works in favour of **3**BF_4 (by 0.4 and 0.8 kcal mol^{-1} at the M05-2X levels and MP2 levels). These calculations qualitatively reproduce the experimental trends: dihydrogen complex favoured in THF and classical dihydride in CH_2Cl_2. The inclusion of three THF molecules provides a relative stabilization of 2.9 kcal mol^{-1} to **2**BF_4, whereas three CH_2Cl_2 molecules only stabilize it by 0.7 kcal/mol. If the cluster formed by the ion-pair and three discrete solvent molecules are solvated with the continuum, the results are only slightly modified.

Concluding this section, the calculations show that ion-paring with the BF_4^- counter-anion energetically stabilizes the dihydrogen complex and the theoretical modelling of the specific solute-solvent interactions suggests that the solvent establishes specific F···H(C) interaction with the anion. The interaction of dichloromethane with the non-classical ion pair, $[Cp^*Mo(CO)(PMe_3)_2(\eta^2\text{-}H_2)]^+BF_4^-$, destabilizes the cation-anion bonding favoring its isomerization to the dihydride form. On the other hand, the weaker interaction with THF is insufficient to perturb the anion-cation interaction and the non-classical form remains favoured as in the gas phase. It is arguable that these effects are responsible for the predominance of a different isomer depending on the solvent.

(c) Protonation of compound 1 by CF_3COOD.

The protonation of **1** was also investigated in THF-d_8 with CF_3COOD, the aim of this study being the generation of complex **2**-d_1 and measuring the $^1J_{HD}$ value. However, the ^1H and $^{31}P\{^1H\}$ NMR spectroscopic monitoring revealed no evidence for the formation of the desired product when using 1 equiv of the acid. The only observable species was compound **1**-*d* as evidenced by an isotopically shifted $^{31}P\{^1H\}$ resonance at δ 32.3 (1:1:1 triplet, $^2J_{PD}$ = 10 Hz). When the amount of acid was increased to 10 equiv, the relative intensity of the **1**-*d* $^{31}P\{^1H\}$ resonance increased, consistent with a greater extent of H/D exchange at the hydride position, but the resonances of **1** in the ^1H and $^{31}P\{^1H\}$ spectra did not disappear. In addition, a broad and weak resonance at δ -4.5 became visible in the ^1H NMR spectrum (*cf.* -5.14 for **2**BF_4). This chemical shift difference can be explained either by a direct counter-ion effect, presumably through hydrogen bonding, $Mo(H_2)\cdots X$, on the proton chemical shift, or by an effect of X on the classical/nonclassical equilibrium position. Unfortunately, the resonance intensity was not sufficient for an accurate T_1 determination.

The lower degree of protonation of **1** by CF_3COOD relative to HBF_4 can be explained by the lower acid strength of the former acid. However, reversible protonation to **2**-d_1 occurs to a sufficient extent to allow the H/D exchange process. Other hydride compounds, for instance $CpRuHL_2$ (L_2 = dppm, dppe, $2PPh_3$), have been shown to be protonated by HBF_4 and not by other relatively strong acids such as TFA, HCl or HBr in THF.[30]

(d) Investigation of the dihydrogen elimination product.

As mentioned above, the dihydrogen elimination from **2** in THF-d_8 or **3** in CD_2Cl_2 occurs above 230 K yielding solutions with very similar spectroscopic properties, see Table 3. When the reaction was carried out in C_6D_6 at room temperature, the ^{31}P NMR spectrum showed a major, broader ($w_{1/2}$ = 10 Hz) peak at δ 17.5 and a minor sharper one at δ 15.5 ($w_{1/2}$ = 4 Hz). When carried out in THF-d_8, the broader resonance ($w_{1/2}$ = 16 Hz) was observed at δ 18.1 while the sharper one was now split into two separate resonances at δ 16.8 and 16.7 in a ca. 2:1 ratio ($w_{1/2}$ = 3 and 4 Hz correspondingly). A THF solution obtained in the same manner showed a visible absorption with a maximum at 510 nm (ε ≈ $2\cdot10^2$ M^{-1} cm^{-1}). The decomposition rate estimated from the IR data at 230 K is essentially the same for **2**

in THF and **3** in CH_2Cl_2 (ca. $2 \cdot 10^{-3}$ s^{-1}), corresponding to an activation free energy $\Delta G^{\neq}_{H2}$ of 16.2 kcal mol^{-1}. This value is much lower than that obtained for the H_2 loss from $[Cp^*MoH_4(dppe)]^+OCOCF_3^-$, yielding $[Cp^*Mo(dppe)H_2(O_2CCF_3)]$ ($\Delta G^{\neq}_{H2}$ = 22.1 kcal mol^{-1} at 270 K).[14] ‡

Possibilities envisaged for the structure of the product are either $[Cp^*Mo(PMe_3)_2(CO)(L)]^+[BF_4]^-$, with L being the solvent (implying that the different donor properties of the two solvents affect the spectroscopic properties of the complex only in a minor way), or $[Cp^*Mo(PMe_3)_2(CO)FBF_3]$ where the BF_4^- anion has entered the metal coordination sphere. The first hypothesis seems reasonable for THF-d_8, which has relatively good coordinating properties, less so for CD_2Cl_2. However, note that complexes where dichloromethane acts as a ligand have been described.[31] The second hypothesis finds precedent in work by Beck *et al.*, describing the formation of the thermolabile complexes $[CpMo(CO)_2(PR_3)FBF_3]$ (R = Ph, OPh, Et) as the products of the reaction between $[CpMoH(CO)_2(PR_3)]$ and $Ph_3C^+BF_4^-$.[32] Note that the protonation of hydride complexes is one of many general methods to access metal complexes of weakly coordinating anions, which are precursors of cationic organometallic Lewis acids.[33]

Table 3. Selected spectroscopic data for the product of H_2 evolution from **2** in THF-d_8 and **3** in CD_2Cl_2 at 230K.

	^{1}H NMR[a]		$^{31}P\{^1H\}$ NMR[a]	$^{13}C\{^1H\}$ NMR[a]	IR
Solvent	δ Cp*	δ PMe_3[b]	δ PMe_3[c]	δ CO[d]	ν_{CO}/cm^{-1}
THF-d_8	1.85 (s)	1.48 (d, 8)	19.4 (quint, 8)	268.7 (t, 31)	1800
CD_2Cl_2	1.88 (s)	1.47 (d, 8)	19.2 (s)	e	1794

[a]Signal multiplicity and relevant coupling constants (Hz) in parentheses. [b]J_{PH}. [c]J_{PF}. [d]J_{CP}. [e]Not detected.

A most enlightening observation comes from the $^{31}P\{^1H\}$ resonance of the sample obtained in THF-d_8 and especially its coupling pattern, featuring a perfect binomial quintet with J = 8 Hz) at 230 K, see Figure 5, and coalescing into a singlet at room temperature. The only possible way to rationalize this coupling pattern is to invoke P-F scalar coupling and therefore BF_4 coordination. However, the observed identical coupling to all F atoms implies a rapid mutual (intramolecular) exchange between the four atoms in the coordination position. This may occur by either an associative or a dissociative mechanism, as shown in Scheme 1. This situation has been previously described for $[CpW(CO)_2\{P(OPh)_3\}(FBF_3)]$[34] and also for complexes containing other weakly coordinating anions, such as $[W(CO)_3(NO)(PMe_3)(FSbF_5)]$.[35] The product of H_2 evolution from either **2** or **3** can therefore be formulated as $[Cp^*Mo(CO)(PMe_3)_2(FBF_3)]$ (**4**). There are numerous crystallographically characterized compounds displaying this coordination mode for the BF_4^- ion, mostly with late transition metals. No X-ray structure has so far been reported for mononuclear complexes of Mo^{II}, but related examples for W^{II} include $W(CO)_3(NO)(PMe_3)(FBF_3)$[36] and $WH(CO)_3(PCy_3)_2(FBF_3)$.[37]

Contrary to the behavior in THF-d_8, the $^{31}P\{^1H\}$ resonance is a singlet at all temperatures in CD_2Cl_2, consistent with a greater extent of dissociation of the ion pair in this solvent, which is expected to better solvate the BF_4^- ion through the establishment of F_3B-F···H-$CHCl_2$ hydrogen bonding[13, 38] (see also the computational work on **2**BF_4···solvent and **3**BF_4···solvent described in section *b* above). This leads to faster i*nter*molecular anion exchange and consequently loss of P-F coupling. However, the similarity of the ν_{CO} frequencies of **4** in the two solvents (Table 3) suggests that the major species present in solution also adopts a molecular geometry in CH_2Cl_2.

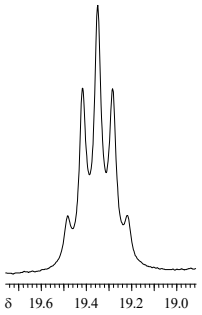

Figure 5. Enlargement of the $^{31}P\{^1H\}$ NMR resonance for the compound obtained from the decomposition of 2 in THF-d_8 at 230K.

It is interesting to compare the rate of mutual F exchange of **4** with that of the previously investigated similar compounds, all of which have at least one additional CO ligand in the coordination sphere, $[CpM(CO)_2(L)(FBF_3)]$.[32, 34, 39] They are most typically at the slow exchange limit at low temperatures, revealing the averaged spectrum only in certain cases at room temperature. In our case, no decoalescence nor any sign of line broadening was noticeable down to 190 K. This comparison shows that the BF_4^- ligand is much more labile in compound **4**, probably for both steric and electronic reasons. The collective behavior of the different compounds appears most consistent with a dissociative exchange mechanism. The shape of this resonance in THF-d_8 changes upon warming, becoming a singlet and shifting upfield on going to ambient temperatures ($\Delta\delta$ = 1.3 ppm between 230 and 298 K). This behavior evidences the onset of an exchange involving more than one ion pair, probably assisted by solvent coordination as shown in Scheme 1, whereby coupling information between a specific Mo atom and a specific BF_4^- group is lost. Again, this is a typical phenomenon already observed for other FBF_3 complexes.[33] Thus, the compound exists at low temperatures in THF-d_8 as an uncharged molecular species, perhaps in equilibrium with a tight ion pair (the dissociative intermediate of the mutual exchange process), but equilibrates at higher temperatures with increasing amounts of the free ions, allowing the intermolecular exchange, see Scheme 1.

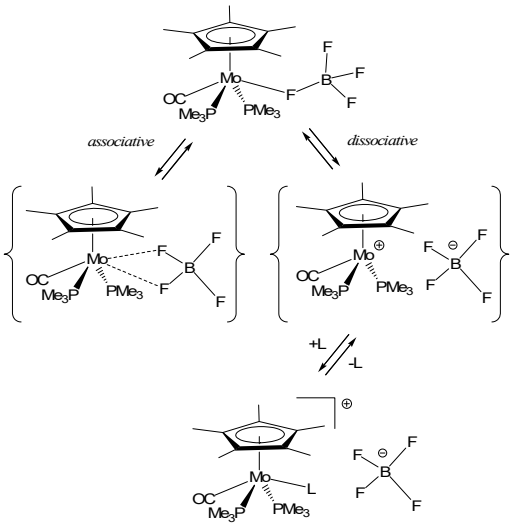

Scheme 1.

(d) Formation and characterization of an HF complex.

Leaving solutions of complex **4**, either in THF-d_8 or in CD_2Cl_2, at ambient temperature for extended periods of time resulted in further decomposition: ^{31}P and ^{13}C NMR monitoring revealed the formation of several products. Upon attempting to crystallize compound **4** prepared *in situ* from **1** and 0.5 eq of $Et_2O{\cdot}HBF_4$ in toluene at ca. 250 K, violet crystals were obtained. An X-ray analysis shows that this corresponds to $[Cp^*Mo(PMe_3)_2(CO)(FH\cdots FBF_3)]$, **5**, namely the coordination position occupied by the BF_4^- anion in compound **4** has been replaced by a neutral HF molecule, which then further binds the BF_4^- anion through a hydrogen bond.

Selected bond distances and angles for the structure of compound **5** are listed in Table 4. In the structure, each anion makes two short F···(HF) contacts with two different cations through atoms F(13) and F(14), while each cation is in close proximity of two different anions, such that the anions and cations are packed in pairs, as shown in Figure 6. Therefore, the proton of the HF ligand must be disordered among two sites, the F1···F13 and F1···F14 vectors. The disordered H atom was in fact directly located in both positions, with the intensity data suggesting a 50:50 distribution (see details in the Experimental Section). The other two F atoms of the anion, F(11) and F(12), do not display any contact with neighboring ions shorter than the van der Waals distances. The four B-F bonds are not equivalent, those involved in the hydrogen bond with HF (B(1)-F(13) and B(1)-F(14)) being the longest. The structure also contains one molecule of interstitial toluene.

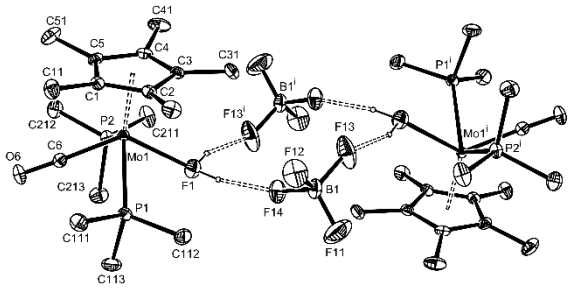

Figure 6. An ORTEP view of the molecular geometry of compound $[Cp^*Mo(PMe_3)_2(CO)(FH\cdots FBF_3)]$, 5, with the atom-labelling scheme showing the formation of a pseudo-dimer through F-H···F hydrogen bonds. Displacement ellipsoids are drawn at the 30% probability level and the disordered H atoms are represented as small spheres of arbitrary radius. Symmetry code: (^{i}) 1-x, 1-y, 1-z.

The coordination geometry of the cation is a typical four-legged piano stool, with one CO, two PMe_3 and an HF molecule as "leg" ligands. The CNT-Mo-L angles are in the narrow 115-122° range. The most interesting structural feature is the hydrogen bonding interaction between the ions. Hydrogen bonds connecting two fluorine atoms in coordination compounds are common when the proton acceptor is metal bound F^-, making up the hydrogen bifluoride $(FHF)^-$ ligand, crystallographically characterized examples being $[M(PMe_3)_4H_2F(FHF)]$ (M = Mo, W),[40] $[Ru(dppe)_2F(FHF)]$,[41] $[Ru(PMe_3)_4H(FHF)]$,[42] $[(COD)Rh(PPh_3)(FHF)]$,[43] and $[Pd(Ph)(PPh_3)_2(FHF)]$,[44] but we find no precedent in the CSD of an HF ligand bonded to a transition metal with an additional H-bond to BF_4^-. In the structures above where the H atom was located, this is placed closer to the dangling F atom than to the metal-coordinated F atom. The structure can therefore be better represented as an HF adduct of a fluorido complex, M-F···H-F, rather than as a cationic HF complex, $[M(F\text{-}H)]^+\cdots F^-$, whereas the disordered H atom in **5** is located closer to the molybdenum bound F atom than to FBF_3 (0.96 vs 1.78 Å), allowing this compound to be better described as a cationic HF complex, $[Cp^*(PMe_3)_2(CO)Mo(FH)]^+\cdots FBF_3^-$. The Mo-F distance in **5** is much longer than the typical terminal Mo^{II}-F bond to a fluorido ligand (average of 2.01(4) Å over 9 distances in 7 structures retrieved from the CDS).[45] The above mentioned $[Mo(PMe_3)_4H_2F(FHF)]$ complex also has a shorter Mo-(FHF) distance (2.124(3) Å) than in our compound, because the fluorine atom bonded to Mo has a greater electron density in $(FHF)^-$ relative to $(FH\cdots FBF_3)^-$. The closest relative to the arrangement of the HF ligand in the structure of **5** are $La(HF)_2(AsF_5)_3$, where intermolecular La-(FH)···(FAsF$_5$)La is observed.[46] It should be mentioned that intramolecular examples of M-(FH)···B moieties (B = proton acceptor such as the 2-NH_2 group of metal-coordinated *o*-aminopyridine) have also been described, though without structural characterization.[47] Comparison of all these results shows that with a proton acceptor as strong as F^-, there is a preference for M-F···H-F, whereas weaker proton donors (neutral NH_2 groups or anionic AsF_6^- and BF_4^-) lead to M-F-H···B.

Table 4. Selected bond distances (Å) and angles (deg) for compound $[Cp^*Mo(PMe_3)_2(CO)(FH\cdots FBF_3)]$, **5**.[a]

CNT(1)-Mo(1)	1.9968(12)	Mo(1)-P(2)	2.4777(7)
Mo(1)-C(6)	1.895(3)	P(1)-C(113)	1.810(3)
C(6)-O(6)	1.177(3)	P(1)-C(111)	1.815(3)
Mo(1)-F(1)	2.2988(16)	P(1)-C(112)	1.825(3)
F(1)-H(1A)	0.96	P(2)-C(213)	1.815(3)
F(1)-H(1B)	0.96	P(2)-C(212)	1.815(3)
F(1)···F(13)	2.697(3)	P(2)-C(211)	1.825(3)
F(1)···F(14)	2.714(2)	B(1)-F(11)	1.325(4)
H(1A)···F(14)	1.78	B(1)-F(12)	1.362(4)
H(1B)···F(13)	1.79	B(1)-F(13)	1.384(4)
Mo(1)-P(1)	2.4672(7)	B(1)-F(14)	1.386(4)
F(1)-H(1A)···F(14)	164	F(12)-B(1)-F(13)	106.3(3)
F(1)-H(1B)···F(13)	157	CNT(1)-Mo(1)-P(1)	120.11(4)
Mo(1)- F(1)-H(1A)	122.0	CNT(1)-Mo(1)-P(2)	121.71(3)
Mo(1)- F(1)-H(1B)	118.0	Mo(1)-F(1)-F(14)	129.18(8)
Mo(1)-F(1)-F(13)^i	130.70(9)	CNT(1) -Mo(1)-F(1)	114.96(6)
P(1)-Mo(1)-P(2)	118.07(2)	CNT(1)-Mo(1)-C(6)	117.72(8)
C(6)-Mo(1)-F(1)	127.32(9)	C(6)-Mo(1)-P(2)	74.76(7)
C(6)-Mo(1)-P(1)	74.51(8)	F(1)-Mo(1)-P(2)	78.74(4)
F(1)-Mo(1)-P(1)	79.35(5)	F(11)-B(1)-F(14)	111.4(3)
O(6)-C(6)-Mo(1)	177.4(2)	F(12)-B(1)-F(14)	108.1(2)
F(11)-B(1)-F(12)	110.8(3)	F(13)-B(1)-F(14)	108.2(3)
F(11)-B(1)-F(13)	111.7(3)		

[a]CNT is the Cp ring centroid. Symmetry code (^{i}): 1-x, 1-y, 1-z.

In the solid state complex **5** displays a ν_{CO} band at 1780 cm^{-1}, i.e. very close to that of compound **4**. Two ν_{BF} bands appear at 937 and 1018 cm^{-1}, accompanied by unresolved bands of lower intensity at ca 1106 and 1163 cm^{-1}, in agreement with the expected lowering of the BF_4^- symmetry. A broad band at 3477 cm^{-1} is assigned to the ν_{HF} stretching vibration. This value is substantially higher than that of the hydrogen bifluoride ion in its various salts (ν_{HF} = 1250–1750 cm^{-1})[48] or in the above mentioned hydrogen bifluoride complexes of transition metals (ν_{HF} = 2310–2793 cm^{-1}).[40b, 41] On the other hand, it is much lower than the ν_{HF} stretching mode for free HF in the gas phase (3960 cm^{-1})[49] or weakly bonded $HF{\cdot}BF_3$ complex (3958 cm^{-1}),[50] being in agreement with an HF bond elongation with respect to free HF (0.918 Å).[40b]

Discussion

Examples of tautomeric pairs of classical dihydride and dihydrogen complexes with very similar energy are rather common.[2] In some cases, the energetic preference was shown to switch by a subtle change in the donor/acceptor and steric properties of other ligands. For instance, complex $[Mo(R_2PCH_2CH_2PR_2)_2(CO)H_2]$ is a classical dihydride when R = Et, *i*Bu and a dihydrogen complex when R = Ph, Bz,[51] while complex $W(CO)_3(PR_3)_2H_2$ shows the two tautomeric forms in equilibrium when R = *i*Pr but is present exclusively as the classical dihydride when R = Me.[52] It has been previously shown that the H-H distance in dihydrogen complexes may be very sensitive to intra- and intermolecular interactions, including ion pairing.[53] In one case, a switch was highlighted for the same cationic complex, $[Co(PP_3)H_2]^+$ [$PP_3 = P(CH_2CH_2PPh_2)_3$], by a mere change of counter-anion in the solid state: the classical dihydride structure is adopted in the presence of the BPh_4 anion, whereas the corresponding PF_6 salt reveals a nonclassical dihydrogen structure (though the position of the two H atoms was not located).[54] An NMR study, on the other hand, only reveals the classical structure in solution.[55] The example herein described, with both cation and anion being invariant and a complete switch *in solution* being caused by a subtle solvent change, appears to be unprecedented.

The overall reaction of **1** with HBF_4 may be described as shown in Scheme 2. The first question to address is whether the predominant formation of **2** in THF and **3** in CH_2Cl_2 has a kinetic or thermodynamic origin. High activation barriers for the interconversion of classical dihydrides and dihydrogen complexes are sometimes observed when the isomerization involves extensive ligand rearrangement. Examples are *cis*-$[Cp^*M(dppe)(\eta^2\text{-}H_2)]^+$/*trans*-$[Cp^*M(dppe)H_2]^+$ ($\Delta H^{\ddagger}$ = 20.4(8), 20.9(8), and 21.5(10) kcal mol^{-1} for M = Fe,[6d] Ru,[7] and Os[56] respectively) and $[W(CO)_3(PR_3)_2(\eta^2\text{-}H_2)]$/$[W(CO)_3(PR_3)_2H_2]$ with R = cyclopentyl ($\Delta G^{\ddagger}$ = 11(2) kcal mol^{-1}).[57] Theoretical investigations have shown that the $M(\eta^2\text{-}H_2)$/*cis*-$M(H)_2$ isomerization has a very small barrier when the rest of the coordination sphere does not undergo significant change.[58] The two hydride ligands in complex **3** occupy *cis* coordination sites as shown in **I**, thus the rearrangement to the non-classical form must involve a very minor rearrangement of the coordination sphere. This proposition is confirmed by DFT calculations. Thus, the nature of the product is determined by thermodynamic factors. This conclusion is also consistent with the lack of observation of **2** during the thermal decomposition of **3** and with the essentially identical decomposition rate for the two isomers at the same temperature. From that rate (ca. 10^{-3} s^{-1} at 230 K), we can derive an activation free energy of 16.5 kcal mol^{-1} at 230 K for the H_2 release process, much larger than the energy barrier for the isomerization process. Thus, the rate limiting step must be the H_2 dissociation from **2**.

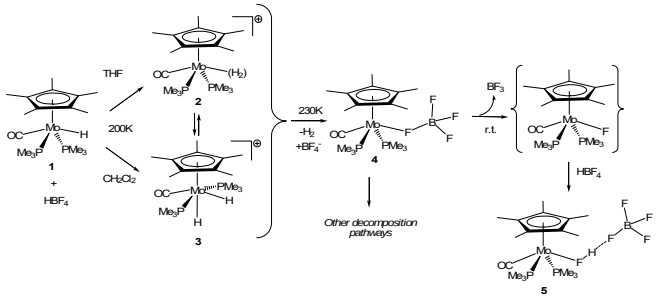

Scheme 2

If the solvent effect is on the thermodynamics and not on the kinetics, the next question to address is what is the origin of this effect, especially considering that THF and CH_2Cl_2 possess similar polarity (dielectric permittivity).[59] The relative stability may be quite small, as little as 1.1 kcal mol^{-1} in favour of **2** in THF and the same amount in favour of **3** in CH_2Cl_2 (*vide supra*). A possibility could be based on the ability of THF to establish H-bonding interactions as a proton acceptor with the H_2 ligand in **2** (supposedly a stronger acid than **3**), whereas dichloromethane rather displays weak proton donating properties and prefers to interact with the BF_4^- anion.[13, 38, 60] However, the computational work suggests that the cations establish much stronger non covalent interactions with the BF_4 counter-anion than with the solvent molecules. Indeed, neither CH_2Cl_2 nor THF break the $[Cp^*(PMe_3)_2(CO)MoH_2]BF_4$ ion pair but merely alter the cation-anion interaction in a rather minor way. Thus, the effect of the solvent on the classical/nonclassical equilibrium energetics can be described as operating through a second-order non covalent interaction: solvent···anion···cation. The computational study, especially with the aid of calibrations by high level MP4(SDQ) and CCSD(T) on a simplified model, suggest that the dihydride isomer is inherently more stable than the dihydrogen complex, though by a very small margin, and that the explicit inclusion of anion and solvent molecules tilts the balance in favour of the dihydrogen complex, to a greater extent in THF than in CH_2Cl_2.

The experimental observations reported in this contribution may be compared with previously published protonation reactions of similar compounds, in order to trace the influence of the ligand environment on the nature and stability of the protonation product. Treatment of $[CpMo(CO)_2(PMe_3)H]$ with $Et_2O{\cdot}HBF_4$ leads to immediate H_2 evolution, even at -78°C in poorly coordinating or non coordinating solvents such as ether, toluene, and heptane.[61] In the presence of sufficiently coordinating solvents (for instance, L = MeCN), stable solvent adducts $[CpMo(CO)_2(PMe_3)(L)]^+$ were obtained. The protonation of $[CpMo(PMe_3)_3H]$[21a] or $[Cp^*Mo(PMe_3)_3H]$[21b] with HBF_4, on the other hand, leads to stable dihydride products, $[(Ring)Mo(PMe_3)_3H_2]^+$ (Ring = Cp or Cp*), showing that the metal center in this compound is sufficiently electron-rich to prevent formation of a $(\eta^2\text{-}H_2)$ complex and H_2 evolution. The present results show that an intermediate electronic environment (only one CO ligand and two PMe_3 ligands, Cp* in place of Cp) is sufficient to stabilize the primary protonation product – non-classical hydride **2** at low temperatures in THF, but not sufficient to prevent H_2 elimination at higher temperatures.

Bullock has reported a low-temperature NMR study of the protonation of complex [CpMo(dppe)(CO)H], which is electronically very similar to compound **1**, with TfOH. The reaction, conducted in CD_2Cl_2, led to the direct formation of the dihydride product, $[CpMo(dppe)(CO)H_2]^+$, without observation of a dihydrogen complex intermediate.[23] This product decomposes with loss of H_2 upon warming with formation of [CpMo(dppe)(CO)(OTf)]. Like the latter system, compound **3** also loses H_2 upon warming with incorporation of the counter-anion and yields **4** (Scheme 2). It is remarkable, in our opinion, that the metal in this compound prefers to accept the weakly coordinating BF_4^- anion rather than a molecule of the THF solvent. Previously described $[CpMo(CO)_2(PR_3)(FBF_3)]$ analogues were apparently always handled in cold CH_2Cl_2 and the BF_4^- ligand was readily substituted by phosphines and olefins,[32] but their behavior in more coordinating solvents does not appear to have been tested. Other compounds containing this and other weakly coordinating anions (PF_6, SbF_6, CF_3SO_3, etc.) have been generated in

hydrocarbon solvents and the weakly coordinating anions were readily displaced under very mild conditions by a number of neutral donors, including weak ones such as R_2O.[33] In the review by Beck and Sünkel, the affinity of $[CpM(CO)_2(L)]^+$ systems (M = Mo, W; L = tertiary phosphine) for Lewis bases is described as $CH_2Cl_2 < BF_4^- < THF$.[33] The different trend observed in our case for system $[Cp^*Mo(CO)(PMe_3)_2]^+$ may be rationalized on steric grounds, since the metal coordination sphere is more crowded in the present system and THF requires more space in the coordination sphere than FBF_3. The formation of complex **5** may be rationalized on the basis of the rupture of the B-F bond with loss of BF_3 from compound **4**, which is promoted by the Lewis acidity of the Mo atom, followed by trapping of the fluoride intermediate by an additional HBF_4 molecule.

Conclusions

The present investigation has shown a striking example of how delicately the ligand environment and the solvent nature control the relative stability of a classical dihydride *vs.* its isomer dihydrogen complex for the protonation product of (Cp')MoL_3H-type molecules. With an electron-rich ligand environment, *e.g.* Cp' = Cp or Cp* and $L_3 = (PMe_3)_3$, stable compounds with a classical dihydride structure are obtained. With an electron poor environment, *e.g.* Cp' = Cp and $L_3 = (CO)_2(PMe_3)$, immediate decomposition occurs at 195 K, probably via a fleeting dihydrogen complex. For compound **1** with intermediate electronic properties, we have shown here for the first time how the reaction can be steered toward the classical or the non classical product by a small change of solvent properties. High level DFT calculations with the inclusion of counter-anion and solvent effects (through the CPCM and also through the explicit introduction of solvent molecules) have revealed intimate details on the organization of the **2**BF_4 and **3**BF_4 ion pairs in solution. A solvent regulation of a classical/nonclassical equilibrium with complete switch *in solution*, where both cation and anion are invariant, appears to be unprecedented. The analysis reported here also unveils that a network of solvent···anion···cation non covalent interactions is responsible for a dramatic change in the cation nature, showing the steering role of specific solute-solvent interactions.

Experimental Section

General. All manipulations were carried out under an argon atmosphere. All solvents were dried over appropriate drying agent (Na/benzophenone for toluene and THF; CaH_2 for dichloromethane) and freshly distilled under an argon atmosphere prior to use. C_6D_6 and toluene-d_8 (Euriso-Top) were kept over molecular sieves and deoxygenated with an argon flow before use. CD_2Cl_2 and THF-d_8 (Euriso-Top) were degassed by three freeze-pump-thaw cycles, then purified by vacuum transfer at room temperature. Compound $[Cp^*Mo(CO)(PMe_3)_2H]$ was synthesized according to the literature procedure.[15] Et_2OHBF_4 (56%, Sigma Aldrich) was used as received.

Instrumentation. Room temperature NMR investigations were carried out on Bruker DPX300 and AV300LiQ spectrometers operating at 300.1 MHz (^{1}H), 121.49 MHz (^{31}P{^{1}H}) and 75.47 MHz (^{13}C{^{1}H}). Low-temperature ^{1}H, ^{31}P{^{1}H} and ^{13}C{^{1}H} data were collected with a Bruker AV500 spectrometer, operating at 500.3, 202.5 and 125.8 MHz, respectively. The temperature was calibrated using a methanol chemical shift thermometer; the accuracy and stability was ±1 K. All samples were allowed to equilibrate at every temperature for at least 3 min. The spectra were calibrated with the residual solvent resonance relative to TMS (^{1}H, ^{13}C), and with external 85% H_3PO_4 (^{31}P). The conventional inversion-recovery-pulse method (180-τ-90) was used to determine the variable-temperature longitudinal relaxation time T_1, the calculations being done with standard Bruker software. The IR spectra were recorded on PerkinElmer Spectrum 100 FT-IR (2.0 cm^{-1} resolution), Specord M-82 (4.0 cm^{-1} resolution) and FT Infralum-801 (2.0 cm^{-1} resolution) spectrometers; 0.12 or 0.04 cm cells were used for solutions.

***In situ* generation of compound 2 and subsequent thermal decomposition.** In a 5 mm NMR tube was added compound **1** (10 mg, 0.024 mmol) followed by THF-d_8 (0.6 mL). After cooling to 200 K, a 56% ether solution of HBF_4 (3 μL, 0.70 equiv from NMR integration) was added by microsyringe and the reaction was monitored directly by NMR probe.

In a separate experiment, the same reaction [5 mg (0.012 mmol) of **1** and ca. 1.5 μL (ca. 0.012 mmol) of the HBF_4 ether solution] was carried out in regular THF (1 mL) in a Schenk tube and the resulting solution was transferred by cannula into the IR cell inside a precooled cryostat, and monitored by IR spectroscopy in the ν_{CO} region.

***In situ* generation of compound 3 and subsequent thermal decomposition.** This experiment was run by an identical protocol as the previous one, using 10 mg (0.024 mmol) of **1** in 0.6 mL of CD_2Cl_2 and 3 μL (0.78 equiv from integration) of the HBF_4 ether solution.

In a separate experiment, the same reaction [5 mg (0.012 mmol) of **1** and ca. 1.5 μL (ca. 0.012 mmol) of the HBF_4 ether solution] was carried out in CH_2Cl_2 (1 mL) in a Schenk tube and the resulting solution was transferred by cannula into the IR cell inside a precooled cryostat, and monitored by IR spectroscopy in the ν_{CO} region.

Generation of compound 5. To a solution of compound **1** (30 mg, 0.07 mmol) in toluene (1 mL) was added a 56% ether solution of HBF_4 (ca. 4.5 μL, ca. 0.035 mmol) by microsyringe at room temperature. A pentane layer (ca. 0.5 mL) was subsequently placed on top of the solution, which was set at -20°C. A few crystals of compound **5** formed in two days. The amount was only sufficient to record an IR spectrum and for an X-ray structural analysis. IR (neat/cm^{-1}): 1780 s (ν_{CO}), 1091 m, 1030 m, 1004 m, 936 s (BF_4^-).

X-Ray Analysis of Compound 5. A single crystal was mounted under inert perfluoropolyether at the tip of a glass fibre and cooled in the cryostream of an Oxford-Diffraction XCALIBUR CCD diffractometer. Data were collected using the monochromatic MoKα radiation (λ= 0.71073). The structure was solved by direct methods (SIR97)[62] and refined by least-squares procedures on F^2 using SHELXL-97.[63] All H atoms attached to carbon were introduced in calculation in idealised positions and treated as riding on their parent atoms. The two positions of the disordered H atom attached to F1 were located in the difference Fourier map and refined first using restraints (F-H= 0.94(1) Å), then treated as riding on the F atom during the last stages of refinement with U_{iso}= 1.2U_{eq}(F). There is one well behaved toluene solvate molecule per asymmetric unit. The drawing of the molecule was realised with the help of ORTEP32.[64] Crystal data and refinement parameters are shown in Table 5. Crystallographic data (excluding structure factors) have been deposited with the Cambridge Crystallographic Data Centre as supplementary publication no. CCDC 714915. Copies of the data can be obtained free of charge on application to the Director, CCDC, 12 Union Road, Cambridge CB2 1EZ, UK (fax: (+44) 1223-336-033; e-mail: deposit@ccdc.cam.ac.uk).

Computational details. All calculations were performed at the DFT level, by means of the M05-2X functional[27] as well as the hybrid B3LYP functional,[65] as implemented in Gaussian03.[66] The optimizations of the dihydrogen/dihydride cations, the ion pairs with the BF_4^- counter-anion, and the adducts containing one solvent molecule were also performed at the DFT/B3PW91 and MP2 levels. The MP4(SDQ) and CCSD(T) methods were used for single-point calculations at the MP2-optimized geometry of the model $[CpMo(CO)(PH_3)_2H_2]^+$ complexes. The basis set for the Mo and P atoms was that associated with the pseudopotential[67] with a standard double-ζ LANL2DZ contraction,[66] supplemented in the case of P with a set of d-polarization functions.[68] The 6-31G(d) basis set was used for C atoms of Cp* ring and CH_2Cl_2 as well as for B and F atoms of BF_4. The 6-31++G(d,p) basis set was used for the CO group, the hydride ligands, the O atom of THF, the CH_2Cl_2 chlorine atoms and the acidic H atoms of HBF_4 and CH_2Cl_2. The 6-31G basis set was used for all other atoms. The structures of the reactants, intermediates, transition states, and products were fully optimized without any symmetry restriction. Transition states were identified by having one imaginary frequency in the Hessian matrix. No scaling factor was applied to the calculated frequencies since the optimization was run in the gas phase and the IR spectra were measured in solution. The average ratio between experimental and calculated ν_{CO} values is ca 0.95. Non-specific solvent effects were introduced through CPCM (conductor-like polarizable continuum model) representation of the solvent by single-point calculations[69] on gas phase optimized geometries for dichloromethane (ε = 8.93) and THF (ε = 7.58). The ΔE^{solv} and ΔG^{solv} values have been obtained adding the contribution of the free energy of solvation to the gas-phase potential energy and gas phase free energy, respectively.[70] Specific solvent effects in the ion pairs were considered by introducing discrete solvent molecules (either CH_2Cl_2 or THF) to solvate the BF_4 anion of the ion pair. To generate good starting points for the optimization of the solvated ion-pairs the most stable conformation of the solvated free BF_4 anion was initially investigated. Then the arrangement of the solvent molecules found was introduced in the most stable conformations of the ion-pairs and the system was fully optimised.

Table 5. Crystal data and structure refinement for $[Cp^*Mo(PMe_3)_2(CO)(FH\cdots FBF_3)]\cdot C_6H_5CH_3$, **5**.[a]

Empirical formula	C_{24} H_{42} B F_5 Mo O P_2
Formula weight	610.27
Crystal colour, habit	dark violet, box
Crystal size (mm)	0.54 x 0.32 x 0.16

Temperature, K	180(2)
Crystal system	Monoclinic
Space group	P 2_1/a
a (Å)	9.6293(3)
b (Å)	26.8813(7)
c (Å)	11.3274(3)
β (°)	100.553(3)
V (Å^3)	2882.48(14)
Z	4
D_{calc} (g cm^{-1})	1.406
Linear absorption, μ (mm^{-1})	0.613
T_{min}/T_{max}	0.43366 / 1.000
θ Range (°)	32.12
F(000)	1264
Reflections measured	30896
Independent reflections [R_{int}]	9529 [0.0438]
Completeness of dataset (%)	94.3
Observed reflections [$I > 2\sigma(I)$]	5715
Parameters	319
GOF	0.984
R1, wR2 [I>2σ(I)]	0.0355, 0.0810
R1, wR2 (all data)	0.0789, 0.0996
$\Delta\rho_{min}$, $\Delta\rho_{max}$ (e Å^{-3})	1.191 , -0.900

[a] Only the average values are given for chemically equivalent parameters. [b] From reference [71].

Acknowledgements

Support of this work through two bilateral programs (France-Russia: PICS grant 2004-07, continuing within the framework of a GDRE (groupe de recherche européen) 2008-11; France-Spain: LEA-CTPMM) is gratefully acknowledged. Additional national support was obtained in France from the CNRS, the IUF, and the CICT (project CALMIP), in Russia from the RFBR (08-03-00464), the Division of Chemistry and Material Sciences of RAS and the Russian Federation President grant (MK-380.2008.3) and in Spain from MICINN (projects CTQ2008-06669-C02-01 and Consolider Ingenio 2010 CSD2007-00006). OAF thanks INTAS for an individual YSF grant (№06-1000014-5809). Thanks are also expressed to Dr. Y. Coppel (LCC CNRS) for assistance with the low temperature NMR measurements.

Supporting Information available

Complete spectroscopic data for compounds **2**, **3**, **4**. Low-T IR spectra in CH_2Cl_2 and THF. Tables and Figures of the DFT results. Cartesian coordinates of all optimized structures.

[1] G. J. Kubas, R. R. Ryan, B. I. Swanson, P. J. Vergamini and H. J. Wassermann, *J. Am. Chem. Soc.* **1984**, *106*, 451-452.

[2] G. J. Kubas, *Metal Dihydrogen and σ-Bond Complexes*, Kluwer Academic/Plenum Press, New York, **2001**, pp.

[3] M. A. Esteruelas and L. A. Oro, *Chem. Rev.* **1998**, *98*, 577-588.

[4] N. K. Szymczak and D. R. Tyler, *Coord. Chem. Rev.* **2008**, *252*, 212-230.

[5] C. P. Lau, S. M. Ng, G. Jia and Z. Lin, *Coord. Chem. Rev.* **2007**, *251*, 2223-2237.

[6] G. J. Kubas, *Chem. Rev.* **2007**, *107*, 4152-4205.

[7] G. J. Kubas, *Acc. Chem. Res.* **1988**, *21*, 120-128.

[8] P. G. Jessop and R. H. Morris, *Coord. Chem. Rev.* **1992**, *121*, 155-284.

[9] P. Hamon, L. Toupet, J.-R. Hamon and C. Lapinte, *Organometallics* **1992**, *11*, 1429-1431.

[10] N. V. Belkova, P. O. Revin, L. M. Epstein, E. V. Vorontsov, V. I. Bakhmutov, E. S. Shubina, E. Collange and R. Poli, *J. Am. Chem. Soc.* **2003**, *125*, 11106-11115.

[11] N. V. Belkova, E. Collange, P. Dub, L. M. Epstein, D. A. Lemenovskii, A. Lledós, O. Maresca, F. Maseras, R. Poli, P. O. Revin, E. S. Shubina and E. V. Vorontsov, *Chem. Eur. J.* **2005**, *11*, 873-888.

[12] M. Baya, O. Maresca, R. Poli, Y. Coppel, F. Maseras, A. Lledós, N. V. Belkova, P. A. Dub, L. M. Epstein and E. S. Shubina, *Inorg. Chem.* **2006**, *45*, 10248-10262.

[13] N. V. Belkova, P. A. Dub, M. Baya and J. Houghton, *Inorg. Chim. Acta* **2007**, *360*, 149–162.

[14] P. A. Dub, N. V. Belkova, K. A. Lyssenko, G. A. Silantyev, L. M. Epstein, E. S. Shubina, J.-C. Daran and R. Poli, *Organometallics* **2008**, *27*, 3307-3311.

[15] M. Besora, A. Lledos and F. Maseras, *Chem. Soc. Rev.* **2009**, *38*, 957-966.

[16] S. Gründeman, S. Ulrich, H.-H. Limbach, N. S. Golubev, G. S. Denisov, L. M. Epstein, S. Sabo-Etienne and B. Chaudret, *Inorg. Chem.* **1999**, *38*, 2550-2551.

[17] M. G. Basallote, M. Feliz, M. J. Fernandez-Trujillo, R. Llusar, V. S. Safont and S. Uriel, *Chem. Eur. J.* **2004**, *10*, 1463-1471.

[18] A. G. Algarra, M. G. Basallote, M. Feliz, M. J. Fernandez-Trujillo, R. Llusar and V. S. Safont, *Chem. Eur. J.* **2006**, *12*, 1413-1426.

[19] N. Belkova, M. Besora, L. Epstein, A. Lledós, F. Maseras and E. Shubina, *J. Am. Chem. Soc.* **2003**, *125*, 7715-7725.

[20] N. V. Belkova, T. N. Gribanova, E. I. Gutsul, R. M. Minyaev, C. Bianchini, M. Peruzzini, F. Zanobini, E. S. Shubina and L. M. Epstein, *J. Mol. Struct.* **2007**, *844*, 115-131.

[21] P. A. Dub, M. Baya, J. Houghton, N. V. Belkova, J. C. Daran, R. Poli, L. M. Epstein and E. S. Shubina, *Eur. J. Inorg. Chem.* **2007**, 2813–2826.

[22] J. H. Shin, D. G. Churchill and G. Parkin, *J. Organomet. Chem.* **2002**, *642*, 9-15.

[23] NMR properties of [Cp*Mo(PMe$_3$)$_2$(CO)Cl]: ^{1}H: δ 1.81 (s, 15H, Cp*), 1.41 (d, 18H, $^2J_{H\text{-}P}$ = 8Hz); ^{31}P{^{1}H}: δ 17.9 (s).

[24] P. J. Desrosiers, L. Cai, Z. Lin, R. Richards and J. Halpern, *J. Am. Chem. Soc.* **1991**, *113*, 4173-4184.

[25] M. T. Bautista, K. A. Earl, P. A. Maltby, R. H. Morris, C. T. Schweitzer and A. Sella, *J. Am. Chem. Soc.* **1988**, *110*, 7031-7036.

[26] L. M. Epstein, N. V. Belkova, E. I. Gutsul and E. S. Shubina, *Polish J. Chem.* **2003**, *77*, 1371-1383.

[27] R. M. Bullock, J.-S. Song and D. J. Szalda, *Organometallics* **1996**, *15*, 2504-2516.

[28] J. C. Fettinger, H.-B. Kraatz, R. Poli, E. A. Quadrelli and R. C. Torralba, *Organometallics* **1998**, *17*, 5767-5775.

[29] M. Baya, P. A. Dub, J. Houghton, J.-C. Daran, R. Poli, N. V. Belkova, E. S. Shubina, L. M. Epstein and A. Lledós, *Inorg. Chem.* **2009**, *48*, 209-220.

[30] M. L. H. Green, A. K. Hughes, P. Lincoln, J. J. Martin-Polo, P. Mountford, A. Sella, L.-L. Wong, J. A. Bandy, T. W. Banks, K. Prout and D. J. Watkin, *J. Chem. Soc., Dalton Trans.* **1992**, 2063-2069.

[31] T.-Y. Cheng, D. J. Szalda, J. Zhang and R. M. Bullock, *Inorg. Chem.* **2006**, *45*, 4712-4720.

[32] N. Legrand, A. Bondon, G. Simonneaux, C. Jung and E. Gill, *FEBS Lett.* **1995**, *364*, 152-156.

[33] W. T. Potter, J. H. Hazzard, M. G. Choc, M. P. Tucker and W. S. Caughey, *Biochemistry* **1990**, *29*, 6283-6295.

[34] J. W. Box and G. M. Gray, *Magn. Reson. Chem.* **1986**, *24*, 527-533.

[35] J. W. Box and G. M. Gray, *Inorg. Chem.* **1987**, *26*, 2774-2778.

[36] Y. Zhao, N. E. Schultz and D. G. Truhlar, *J. Chem. Theory Comput.* **2006**, *2*, 364-382.

[37] Y. Zhao and D. G. Truhlar, *Theor. Chem. Acc.* **2008**, *120*, 215-241.

[38] After inclusion of the BF_4^- counter-anion, these alternative geometries are even higher than the global minimum (>10 kcal mol^{-1}).

[39] M. G. Basallote, J. Durán, M. J. Fernández-Trujillo and M. A. Máñez, *Organometallics* **2000**, *19*, 695-698.

[40] M. R. Colsman, T. D. Newbound, L. J. Marschall, M. D. Noirot, M. M. Miller, G. P. Wulfsberg, J. S. Frye, O. P. Anderson and S. H. Strauss, *J. Am. Chem. Soc.* **1990**, *112*, 2349-2362.

[41] S. H. Strauss, *Chemtracts Inorg. Chem.* **1994**, *6*, 1-13.

[42] K. Sünkel, H. Ernst and W. Beck, *Z. Naturforsch.* **1981**, *36b*, 474-481.

[43] W. Beck and K. Sünkel, *Chem. Rev.* **1988**, *88*, 1405-1421.

[44] K. Sünkel, G. Urban and W. Beck, *J. Organomet. Chem.* **1983**, *252*, 187-194.

[45] W. H. Hersh, *J. Am. Chem. Soc.* **1985**, *107*, 4599-4601.

[46] R. V. Honeychuck and W. H. Hersh, *Inorg. Chem.* **1989**, *28*, 2869-2886.

[47] L. S. Van Der Sluys, K. A. Kubat-Martin, G. J. Kubas and K. G. Caulton, *Inorg. Chem.* **1991**, *30*, 306-310.

[48] A. Allerhand and P. V. Schleyer, *J. Am. Chem. Soc.* **1963**, *85*, 1715-1723.

[49] M. Appel and W. Beck, *J. Organomet. Chem.* **1987**, *319*, C1-C4.

[50] V. J. Murphy, T. Hascall, J. Y. Chen and G. Parkin, *J. Am. Chem. Soc.* **1996**, *118*, 7428-7429.

[51] V. J. Murphy, D. Rabinovich, T. Hascall, W. T. Klooster, T. F. Koetzle and G. Parkin, *J. Am. Chem. Soc.* **1998**, *120*, 4372-4387.

[52] N. A. Jasim, R. N. Perutz, S. P. Foxon and P. H. Walton, *J. Chem. Soc., Dalton Trans.* **2001**, 1676-1685.

[53] M. K. Whittlesey, R. N. Perutz, B. Greener and M. H. Moore, *Chem. Commun.* **1997**, 187-188.

[54] J. Vicente, J. Gil-Rubio, D. Bautista, A. Sironi and N. Masciocchi, *Inorg. Chem.* **2004**, *43*, 5665-5675.

[55] D. C. Roe, W. J. Marshall, F. Davidson, P. D. Soper and V. V. Grushin, *Organometallics* **2000**, *19*, 4575-4582.

[56] T. Chandler, G. R. Kriek, A. M. Greenaway and J. H. Enemark, *Crystal Structure Communications* **1980**, *9*, 557-562.

[57] S. J. N. Burgmayer and J. L. Templeton, *Inorg. Chem.* **1985**, *24*, 2224-2230.

[58] R. Ellis, R. A. Henderson, A. Hills and D. L. Hughes, *J. Organomet. Chem.* **1987**, *333*, C6-C10.

[59] J. J. R. Fraústo Da Silva, M. A. Pellinghelli, A. J. L. Pombeiro, R. L. Richards, A. Tiripicchio and Y. Wang, *J. Organomet. Chem.* **1993**, *454*, C8-C10.

[60] Y. Wang, J. J. R. Fraústo Da Silva, A. J. L. Pombeiro, M. A. Pellinghelli, A. Tiripicchio, R. A. Henderson and R. L. Richards, *J. Chem. Soc., Dalton Trans.* **1995**, 1183-1191.

[61] F. V. Cochran, P. J. Bonitatebus and R. R. Schrock, *Organometallics* **2000**, *19*, 2414-2416.

[62] L. Coue, L. Cuesta, D. Morales, J. A. Halfen, J. Perez, L. Riera, V. Riera, D. Miguel, N. G. Connelly and S. Boonyuen, *Chem. Eur. J.* **2004**, *10*, 1906-1912.

[63] Z. Mazej, H. Borrmann, K. Lutar and B. Zemva, *Inorg. Chem.* **1998**, *37*, 5912-5914.

[64] D. H. Lee, H. J. Kwon, P. P. Patel, L. M. Liable-Sands, A. L. Rheingold and R. H. Crabtree, *Organometallics* **1999**, *18*, 1615-1621.

[65] E. Clot, O. Eisenstein and R. H. Crabtree, *New J. Chem.* **2001**, *25*, 66-72.

[66] B. S. Ault, *Acc. Chem. Res.* **1982**, *15*, 103-109.

[67] D. G. Tuck, *Progr. Inorg. Chem.* **1968**, *9*, 161-194.

[68] K. Nauta, R. E. Miller, G. T. Fraser and W. J. Lafferty, *Chem. Phys. Lett.* **2000**, *322*, 401-406.

[69] G. J. Kubas, R. R. Ryan and D. A. Wrobleski, *J. Am. Chem. Soc.* **1986**, *108*, 1339-1341.

[70] G. J. Kubas, R. R. Ryan and C. J. Unkefer, *J. Am. Chem. Soc.* **1987**, *109*, 8113-8115.

[71] G. J. Kubas, C. J. Burns, J. Eckert, S. W. Johnson, A. C. Larson, P. J. Vergamini, C. J. Unkefer, G. R. K. Khalsa, S. A. Jackson and O. Eisenstein, *J. Am. Chem. Soc.* **1993**, *115*, 569-581.

[72] G. J. Kubas, *Comments Inorg. Chem.* **1988**, *7*, 17-40.

[73] D. G. Gusev, *J. Am. Chem. Soc.* **2004**, *126*, 14249-14257.

[74] C. Bianchini, C. Mealli, M. Peruzzini and F. Zanobini, *J. Am. Chem. Soc.* **1992**, *114*, 5905-5906.

[75] D. M. Heinekey, A. Liegeois and M. Van Room, *J. Am. Chem. Soc.* **1994**, *116*, 8388-8389.

[76] D. M. Heinekey and M. Van Roon, *J. Am. Chem. Soc.* **1996**, *118*, 12134-12140.

[77] P. A. Dub, N. V. Belkova, O. A. Fillipov, G. A. Silantyev, J.-C. Daran, L. M. Epstein, R. Poli and E. S. Shubina, **in preparation**.

[78] G. R. K. Khalsa, G. J. Kubas, C. J. Unkefer, L. S. Van Der Sluys and K. A. Kubat-Martin, *J. Am. Chem. Soc.* **1990**, *112*, 3855-3860.

[79] F. Maseras, A. Lledós, E. Clot and O. Eisenstein, *Chem. Rev.* **2000**, *100*, 601-636.

[80] C. Reichardt, *Solvents and Solvent Effects in Organic Chemistry*, WILEY-VCH, Weinheim, **2003**, pp.

[81] A. Fujii, K. Shibasaki, T. Kazama, R. Itaya, N. Mikami and S. Tsuzuki, *Phys. Chem. Chem. Phys.* **2008**, *10*, 2836-2843.

[82] E. A. Quadrelli, H.-B. Kraatz and R. Poli, *Inorg. Chem.* **1996**, *35*, 5154-5162.

[83] A. Altomare, M. Burla, M. Camalli, G. Cascarano, C. Giacovazzo, A. Guagliardi, A. Moliterni, G. Polidori and R. Spagna, *J. Appl. Cryst.* **1999**, *32*, 115-119.

[84] G. M. Sheldrick, *SHELXL97. Program for Crystal Structure refinement*, University of Göttingen, Göttingen, Germany, **1997**, pp.

[85] L. J. Farrugia, *J. Appl. Crystallogr.* **1997**, *32*, 565.

[86] A. D. Becke, *J. Chem. Phys.* **1993**, *98*, 5648-5652.

[87] C. T. Lee, W. T. Yang and R. G. Parr, *Phys. Rev. B* **1988**, *37*, 785-789.

[88] P. Stephens, F. Devlin, C. Chabalowski and M. Frisch, *J. Phys. Chem.* **1994**, *98*, 11623-11627.

[89] M. J. Frisch, G. W. Trucks, H. B. Schlegel, G. E. Scuseria, M. A. Robb, J. R. Cheeseman, J. Montgomery, J. A., T. Vreven, K. N. Kudin, J. C. Burant, J. M. Millam, S. S. Iyengar, J. Tomasi, V. Barone, B. Mennucci, M. Cossi, G. Scalmani, N. Rega, G. A. Petersson, H. Nakatsuji, M. Hada, M. Ehara, K. Toyota, R. Fukuda, J. Hasegawa, M. Ishida, T. Nakajima, Y. Honda, O. Kitao, H. Nakai, M. Klene, X. Li, J. E. Knox, H. P. Hratchian, J. B. Cross, C. Adamo, J. Jaramillo, R. Gomperts, R. E. Stratmann, O. Yazyev, A. J. Austin, R. Cammi, C. Pomelli, J. W. Ochterski, P. Y. Ayala, K. Morokuma, G. A. Voth, P. Salvador, J. J. Dannenberg, V. G. Zakrzewski, S. Dapprich, A. D. Daniels, M. C. Strain, O. Farkas, D. K. Malick, A. D. Rabuck, K. Raghavachari, J. B. Foresman, J. V. Ortiz, Q. Cui, A. G. Baboul, S. Clifford, J. Cioslowski, B. B. Stefanov, G. Liu, A. Liashenko, P. Piskorz, I. Komaromi, R. L. Martin, D. J. Fox, T. Keith, M. A. Al-Laham, C. Y. Peng, A. Nanayakkara, M. Challacombe, P. M. W. Gill, B. Johnson, W. Chen, M. W. Wong, C. Gonzalez and J. A. Pople, *Gaussian 03, Revision D.01*, Gaussian, Inc., Wallingford CT, **2004**, pp.

[90] P. J. Hay and W. R. Wadt, *J. Chem. Phys.* **1985**, *82*, 270-283.

[91] W. R. Wadt and P. J. Hay, *J. Chem. Phys.* **1985**, *82*, 284-298.

[92] A. Höllwarth, M. Böhme, S. Dapprich, A. Ehlers, A. Gobbi, V. Jonas, K. Kohler, R. Stegmann, A. Veldkamp and G. Frenking, *Chem. Phys. Lett.* **1993**, *208*, 237-240.

[93] V. Barone and M. Cossi, *J. Phys. Chem. A* **1998**, *102*, 1995-2001.

[94] M. Cossi, N. Rega, G. Scalmani and V. Barone, *J. Comput. Chem.* **2003**, *24*, 669-681.

[95] A. A. C. Braga, G. Ujaque and F. Maseras, *Organometallics* **2006**, *25*, 3647-3658.

[96] R. C. Elder, *Inorg. Chem.* **1968**, *7*, 1117-1123.

Received: ((will be filled in by the editorial staff))
Revised: ((will be filled in by the editorial staff))
Published online: ((will be filled in by the editorial staff))